9-2011

Single Molecule Analysis of the Arabidopsis FRA1 Kinesin Shows that It Is a Functional Motor Protein with Unusually High Processivity

Chuanmei Zhu

Ram Dixit
Washington University in St Louis, ramdixit@WUSTL.EDU

TITLE: Single molecule analysis of the *Arabidopsis* FRA1 kinesin shows that it is a functional motor protein with unusually high processivity.

Chuanmei Zhu and Ram Dixit

Biology Department, Washington University, St. Louis, 63130.

ABSTRACT (<200 words)

The *Arabidopsis* FRA1 kinesin contributes to the organization of cellulose microfibrils through an unknown mechanism. The cortical localization of this kinesin during interphase raises the possibility that it transports cell wall-related cargoes along cortical microtubules that either directly or indirectly influence cellulose microfibril patterning. To determine if FRA1 is an authentic motor protein, we combined bulk biochemical assays and single molecule fluorescence imaging to analyze the motor properties of recombinant, GFP-tagged FRA1 containing the motor and coiled-coil domains (designated as FRA1(707)-GFP). We found that FRA1(707)-GFP binds to microtubules in an ATP-dependent manner and that its ATPase activity is dramatically stimulated by the presence of microtubules. Using single molecule studies, we found that FRA1(707)-GFP moves processively along microtubule tracks at a velocity of about 0.4 μm/s. In addition, we found that FRA1(707)-GFP is a microtubule plus-end-directed motor and that it moves along microtubules as a dimer. Interestingly, our single molecule analysis shows that the processivity of FRA1(707)-GFP is at least twice the processivity of conventional kinesin, making FRA1 the most processive kinesin to date. Together, our data show that FRA1 is a bona fide motor protein that has the potential to drive long-distance transport of cargo along cortical microtubules.

KEY WORDS: Kinesin, FRA1, cortical microtubule, single molecule, cellulose, *Arabidopsis*.

BACKGROUND

The cell wall controls plant cell morphogenesis by determining the extent and direction of turgor-driven cell expansion and provides mechanical support for the plant body (Cosgrove, 2005; Szymanski and Cosgrove, 2009). The cell wall is composed primarily of polysaccharides including cellulose microfibrils, hemicelluloses and pectins along with a small amount of proteins (Cosgrove, 2005; Sandhu et al., 2009). The cellulose microfibrils make up the core of the cell wall structure and are also the major strength-determining components of the cell wall. Therefore, the spatial organization of the cellulose microfibrils greatly impacts the assembly and function of the cell wall. For example, in the primary walls of rapidly elongating cells, the net orientation of the cellulose microfibrils typically determines the direction of cell expansion (Baskin, 2005). Similarly, the organization of the cellulose microfibrils within specific layers of the secondary cell walls is thought to be important for mechanical strength (Harada and Cote, 1985). How the orderly arrangement of cellulose microfibrils is achieved in both primary and secondary cell walls remains unclear.

The cortical microtubule cytoskeleton, which is located beneath the plasma membrane, is known to play a critical role in regulating the organization of cellulose microfibrils (Endler and Persson, 2011; Lloyd and Chan, 2008; Lucas and Shaw, 2008). The orientation of cellulose microfibrils is typically coincident with that of cortical microtubules and disruption of the cortical microtubule array typically disrupts cellulose organization (Baskin, 2001; Wasteneys and Ambrose, 2009). Live-cell imaging experiments have shown that the plasma membrane-embedded cellulose synthase (CESA) complexes move along linear paths that are coincident with the underlying cortical microtubule tracks (Paredez et al., 2006). Furthermore, when cortical microtubules are experimentally induced to reorient, the CESA trails also concomitantly reorient

(Paredez et al., 2006). Together, these findings suggest that the cortical microtubules somehow guide the direction of movement of the CESA complexes.

The cortical microtubule array also appears to play a role in targeting the insertion of CESA complexes in the plasma membrane, since new CESA complexes at the plasma membrane are observed to appear preferentially along cortical microtubules (Crowell et al., 2009; Gutierrez et al., 2009). One possible mechanism for this targeting activity is that Golgi-derived vesicles bearing CESA complexes are transported along cortical microtubules en route to fusion with the plasma membrane (Crowell et al., 2010; Endler and Persson, 2011; Wightman and Turner, 2010). Cortical microtubules may play a similar role in positioning the delivery of vesicles containing hemicelluloses, pectins and cell wall proteins that contribute to cellulose microfibril organization (Cosgrove, 2005; Geisler et al., 2008).

The directional movement of cellular cargo along microtubule tracks is driven by microtubule-based motor proteins such as kinesins. Kinesins are mechanochemical proteins that use the energy from ATP hydrolysis to perform work such as transport of cargo ranging from molecules to organelles along microtubule tracks. Conceptually, a kinesin that walks along cortical microtubules carrying cell wall-related cargo would be ideally suited to convey the cortical microtubule pattern to the cell wall. The *Arabidopsis* Fragile-fiber 1 (FRA1) kinesin-like protein is an attractive candidate for this function. Loss-of-function mutations of the *FRA1* gene result in disorganized cellulose microfibrils in the secondary cell walls of interfascicular fiber cells (Zhong et al., 2002). Importantly, the cortical microtubule organization is unaffected in the *fra1* mutants (Zhong et al., 2002), indicating that the defective cellulose microfibril organization is not the product of aberrant cortical microtubule arrays. Notably, the FRA1 protein localizes to the cell cortex during interphase (Zhong et al., 2002), which raises the possibility that it might

move along cortical microtubules. However, actual motor function of FRA1 has not been demonstrated.

To determine whether FRA1 is an authentic motor protein, we studied the motor activity of a bacterially expressed truncated version of FRA1 containing its N-terminal motor and coiled-coil domains fused to the green fluorescent protein (GFP). Using bulk biochemical assays and single molecule fluorescence imaging, we show that FRA1 is a bona fide motor that moves as a dimer towards the plus-end of microtubules. In addition, our analysis of the run lengths of individual molecules shows that FRA1 has ultra-high processivity. Taken together, these findings provide direct evidence that FRA1 is a functional motor that is capable of supporting long-distance transport along cortical microtubule tracks.

RESULTS

FRA1(707)-GFP binds to microtubules in an ATP-dependent manner

Bioinformatic analysis of the FRA1 protein indicates the presence of an N-terminal motor domain followed by a long coiled-coil region and tail domain (Zhong et al., 2002) (Figure 1A). The motor domain of kinesins is responsible for binding to microtubules and hydrolyzing ATP while the coiled-coil and tail domains are thought to mediate dimer formation and cargo binding, respectively (Vale, 2003). The motor and coiled-coil domains are known to be sufficient to study kinesin motor activity (Vale and Milligan, 2000). Therefore, to investigate the motor properties of FRA1 *in vitro*, we purified a recombinantly expressed truncated version of FRA1 containing its motor and coiled-coil domains (first 707 amino-acids of FRA1) that was fused to GFP at the C-terminus (Figure 1A). This protein was designated FRA1(707)-GFP. To determine whether

FRA1(707)-GFP is capable of binding to microtubules, we performed microtubule co-sedimentation assays (Figure 1B). We found that FRA1(707)-GFP binds to microtubules in an ATP-dependent manner, which is consistent with previous data that was obtained using only the motor domain of FRA1 (Zhong et al., 2002).

FRA1(707)-GFP is a microtubule-activated ATPase

The basal ATPase activity of kinesins is stimulated upon binding to microtubules (Kuznetsov and Gelfand, 1986). To examine whether FRA1(707)-GFP hydrolyzes ATP and whether this activity is stimulated by microtubules, we measured the steady-state ATPase activity of FRA1(707)-GFP at various microtubule concentrations (Figure 1C). FRA1(707)-GFP has a low ATPase activity in the absence of microtubules ($0.162 \pm 0.064\ s^{-1}$). However, in the presence of microtubules, the ATPase activity of FRA1(707)-GFP is enhanced by about 37-fold ($5.930 \pm 1.055\ s^{-1}$). The $K_{0.5\ (MT)}$ value of FRA1(707)-GFP is about 0.4 μM (Figure 1C), similar to that of conventional kinesin (Case et al., 2000). These results show that FRA1(707)-GFP is a microtubule-stimulated ATPase.

FRA1(707)-GFP moves along microtubules with unusually high processivity

To examine whether FRA1(707)-GFP is capable of moving along microtubules, we used total internal reflection fluorescence (TIRF) microscopy to visualize individual FRA1(707)-GFP molecules along taxol-stabilized, rhodamine-labeled microtubules (Figure 2A). Single molecule imaging has several advantages over traditional bulk methods to analyze kinesin motility: i) it reveals the full distribution of motor activities instead of reporting only the average behavior of a population; and ii) it directly reports key motor properties such as velocity, directionality and

processivity (i.e., the ability of kinesin to take multiple coordinated steps before detaching from a microtubule track).

We conducted two-color, time-lapse TIRF microscopy to image both FRA1(707)-GFP molecules and rhodamine-labeled microtubules. Our time-lapse movies show that individual FRA1(707)-GFP molecules move along microtubules smoothly and unidirectionally in the presence of ATP (Figure 2B, 2C and Supplementary Movie 1). We used kymograph analysis to measure the velocity and processivity of individual FRA1(707)-GFP molecules (Figure 2C). Our data show that FRA1(707)-GFP moves at an average velocity of about 0.40 μm/s (Figure 2D), which is comparable to the velocity reported for other motile kinesins (Woehlke and Schliwa, 2000). In our hands, the average velocity of the human conventional kinesin (HsKin1) is about 0.58 μm/s (Supplementary Figure 1A).

The run length of a kinesin molecule is a direct measure of its processivity of movement. We found that the average run length of FRA1(707)-GFP is about 3.45 μm (Figure 2E), which is two-fold greater than the reported run length for the highly processive conventional kinesin (Vale et al., 1996). In our hands, the average run length of the human conventional kinesin is about 1.93 μm (Supplemental Figure 1B). These results indicate that FRA1(707)-GFP has extremely high processivity.

FRA1(707)-GFP is a microtubule plus-end directed motor

The N-terminal location of the motor domain of FRA1 predicts that FRA1 moves towards the plus-end of microtubules (Lee and Liu, 2004). To test this prediction, we studied the motility of individual FRA1(707)-GFP molecules on polarity-marked microtubules that were generated by using N-ethylmaleimide-treated tubulin to specifically block microtubule

polymerization from the minus-ends (Hyman et al., 1991). We found that FRA1(707)-GFP consistently shows plus-end directed movement (Figure 3; Supplementary Movie 2), as expected from the bioinformatic analysis.

FRA1(707)-GFP functions as a dimer

The presence of a long central coiled-coil domain in the FRA1 polypeptide chain suggests that FRA1 walks as a dimer on the microtubule lattice. To determine whether FRA1 forms a dimer, we conducted photobleaching experiments of individual FRA1(707)-GFP molecules that were bound to microtubules. To prevent unbinding of FRA1(707)-GFP from microtubules upon ATP hydrolysis, we conducted these experiments in the presence of adenylyl-imidodiphosphate (AMP-PNP), a non-hydrolyzable analog of ATP that immobilizes kinesins on microtubules (Lasek and Brady, 1985). For these experiments, we used human conventional kinesin as positive control since it is known to function as a dimer (Adio et al., 2006). We found that the distribution of bleach steps for FRA1(707)-GFP is similar to that of the dimeric conventional kinesin (Figure 4), indicating that FRA1(707)-GFP functions as a dimer.

DISCUSSION

Our data shows that the *Arabidopsis* FRA1 kinesin is a bona fide plus-end directed motor protein that moves as a dimer with unusually high processivity. Given its cortical localization in the cell (Zhong et al., 2002), our data support the hypothesis that FRA1 moves along cortical microtubules and transports cell wall-related cargo over long distances.

The *Arabidopsis* FRA1 kinesin belongs to the kinesin-4 group of the kinesin superfamily (Zhong et al., 2002). Kinesin-4 members in animals serve many functions including chromosome movement during mitosis, anterograde transport in axons, virus infection and DNA damage responses (Bisbal et al., 2009; Martinez et al., 2008; Wu et al., 2008; Zhu and Jiang, 2005). In *Arabidopsis*, FRA1 plays a distinct role in mediating cellulose microfibril organization (Zhong et al., 2002). The *Arabidopsis* genome encodes two other Kinesin-4 members (At3g50240 and At5g60930) that share 48-60% amino-acid sequence identity with FRA1 (Zhong et al., 2002). It remains to be seen whether these two FRA1-like proteins also contribute to cell wall biogenesis. In rice, the FRA1 homolog, called BC12, was recently shown to also contribute to cellulose microfibril deposition (Li et al., 2011; Zhang et al., 2010). Therefore, the function of FRA1 in cellulose microfibril patterning is probably conserved in monocots and dicots. In addition to controlling cellulose organization, the rice *BC12* gene also appears to regulate cell-cycle progression and the biosynthesis of gibberellins (Li et al., 2011; Zhang et al., 2010) . Therefore, FRA1 homologs in other plants may have acquired additional functions besides the core function of controlling cellulose patterning.

The measured FRA1 ATP turnover rate in our bulk ATPase assay is about 6 s^{-1}. This is about 8-fold lower than the expected ATPase rate based on the average velocity of FRA1 (0.4 μm/s) in our single molecule assays. This discrepancy is probably because a portion of the FRA1(707)-GFP kinesin is proteolyzed (Figure 1B) and/or dead, and is therefore inactive. These inactive FRA1 molecules would predictably be immotile and thus would not be counted in our single molecule analyses. In contrast, the inactive FRA1 molecules contribute to the calculation of the ATPase rate in the bulk assay. Therefore, we have probably underestimated the ATPase rate of FRA1 in the bulk ATPase assay.

Although the velocity of FRA1 is comparable to that of other plus-end-directed kinesins, the run length of FRA1 is at least twice than that of conventional kinesin (i.e., kinesin-1), which is known to be a highly processive motor. Therefore, FRA1 has unusually high processivity. We saw a small fraction (about 3%) of FRA1 molecules that moved over distances of 10 µm. These extremely long runs do not lead to an over-estimation of the run length of FRA1, because even if we ignore all runs longer than 10 µm, we still obtain an average run length of 3.43 ± 0.24 µm. Processivity is typically critical for kinesin function. For example, the high processivity of kinesin-1 is important to drive efficient long-distance transport of cargo along axonal microtubules (Gunawardena and Goldstein, 2004; Hirokawa and Takemura, 2005). Therefore, it is reasonable to speculate that the ultra-high processivity of FRA1 is necessary for efficient long-distance transport of cell wall-related cargo along cortical microtubules.

The molecular basis for the high processivity of FRA1 is unknown. Kinesin processivity is determined by features outside of the motor domain such as the net charge of the neck coiled-coil domain (Thorn et al., 2000) and the length of the neck-linker domain (Shastry and Hancock, 2010). Whether these elements are responsible for the high processivity of FRA1 remains to be determined.

One potential mechanism through which FRA1 controls cellulose deposition might be to link the movement of plasma-membrane-embedded CESA complexes to cortical microtubules. As the movement of CESA complexes within the plasma membrane is thought to be driven by the free energy released during the polymerization and crystallization of glucan chains during cellulose microfibril formation (Diotallevi and Mulder, 2007; Herth, 1980), it is unlikely that FRA1 is required to drive the movement of CESA complexes. Rather, FRA1 may act as dynamic

linkers between motile CESA complexes and cortical microtubules, thereby assuring that CESA complexes move along directions defined by the cortical microtubule tracks.

In living cells, CESA complexes within the plasma membrane move at an average velocity of about 330 nm/min (Paredez et al., 2006), which is much slower than the average speed of FRA1(707)-GFP (0.40 μm/s) observed in our *in vitro* motility assays. If plasma-membrane-embedded CESA complexes are cargoes for FRA1, then the speed of FRA1 movement in cells is likely to be slower either due to regulatory mechanisms (Verhey and Hammond, 2009) and/or due to retarding forces exerted by the large, membrane-inserted CESA complex. Physical forces are known to significantly reduce the velocity of kinesins (Svoboda and Block, 1994; Valentine and Block, 2009).

Other potential cargo of FRA1 are Golgi-derived vesicles carrying either CESA complexes, matrix polysaccharides or wall proteins. Transport of these vesicles along cortical microtubules by FRA1 would assure their linear deposition, which might be important to the spatial organization of cellulose microfibrils. Identifying FRA1 cargo will be essential to understand how it regulates cellulose patterning.

MATERIALS AND METHODS

FRA1(707)-GFP construct and protein purification

The *FRA1*(707)-GFP construct was assembled using PCR with the following primers: 5' FRA1(707), CCATGGAATCTACGCCGCCAC; 3' FRA1(707), GAATTCAGATGATTTTCGAGCTTCTAAC; 5'GFP, GAATTCATGGTGAGCA

AGGGCGAG; 3'GFP, CTCGAGCTTGTAC AGCTCGTCCA TG. This construct was confirmed by sequencing and subsequently cloned into the pET-28a vector which introduces a 6xHis-tag at the C-terminal end of the protein. The His-tagged FRA1(707)-GFP was induced to express in BL21 (DE3) Rosetta *Escherichia coli* using 0.4mM IPTG at 20°C for 6 hours and it was purified on a Ni-NTA resin affinity column (Qiagen). The purified fusion protein was then desalted using a PD-10 column (Amersham Biosciences) and exchanged into MAB buffer (10 mM PIPES, 50 mM potassium acetate, 4 mM $MgSO_4$, 1 mM EGTA, pH = 7.0) supplemented with 50 mM NaCl. The purified protein was flash frozen and stored at -80 °C in small aliquots.

Microtubule co-sedimentation assay

Microtubules were assembled from unlabeled bovine tubulin (Cytoskeleton, Denver, CO) in BRB80 buffer (80 mM PIPES, 2 mM $MgCl_2$, 1 mM EGTA, pH = 6.8) containing 1mM Mg-GTP at 37°C for 30 min and then stabilized by adding 40 µM taxol. The microtubule binding assay was performed in a 50 µl reaction containing 1 µM FRA1(707)-GFP with or without 5 µM taxol-stabilized microtubules in BRB80 buffer containing 20 µM taxol. To test the ATP dependence of FRA1 binding to microtubules, 5 mM ATP or 5 mM AMPPNP was included in the reaction. The reaction mixture was incubated at room temperature for 30 min and then centrifuged at 30,000g for 20 min at room temperature to sediment microtubules. The supernatant and pellet fractions were analyzed by SDS-PAGE and the proteins were visualized by Coomassie Brilliant Blue R250 (Sigma, St. Louis, MO).

ATPase assay

ATPase activity of FRA1(707)-GFP was performed using the ATPase/GTPase ELIPA biochem kit (Cytoskeleton, Inc., Denver, CO). Each reaction contains 0.1 µM FRA1(707)-GFP,

0.2 mM 2-amino-6-mercapto-7-methylpurine riboside (MESG), 0.3U purine nucleoside phosphorylase (PNP), 20 μM taxol and 1mM ATP in reaction buffer (15mM PIPES, 5mM $MgCl_2$, pH = 7.0). This assay is based upon an absorbance shift (from 340nm to 360nm) that occurs when MESG is converted to 2-amino-6mercapto-7-methyl purine in the presence of inorganic phosphate by the enzyme PNP. A standard curve for the inorganic phosphate is used to calculate to the amount of phosphate released as measured by the absorbance at 360nm. To measure the ATPase activity in the presence of microtubules, different concentrations of taxol-stabilized microtubules were tested. The absorption of each reaction was measured by a plate reader at 360nm. Three independent experiments were performed.

Single molecule motility assays

Rhodamine-labeled microtubules were assembled in the same way as unlabeled microtubules except using unlabeled tubulin and rhodamine-labeled tubulin at a ratio of 25:1. The *in vitro* motility experiments were conducted as described previously (Ross and Dixit, 2010). Briefly, flow cells (15 μL volume) were constructed using glass slides and silanized coverslips that were attached with double-sided adhesive tape. The flow cell was coated with 0.2% monoclonal anti-tubulin antibody (clone Tub 2.1, Sigma) and then blocked with 5% Pluronic F-127 (Sigma). Then, 120 mM rhodamine-labeled microtubules in MAB buffer containing 20 μM taxol were introduced into the flow cell and the unbound microtubules were washed away by MAB buffer containing 20 μM taxol. Lastly, a motility mix containing 10 nM of FRA1(707)-GFP, 1mM Mg-GTP, 50 mM DTT and an oxygen-scavenging system consisting of glucose oxidase and glucose is flowed in. For the experiments to study the directionality of FRA1(707)-GFP, polarity-marked microtubules were generated as described previously (Hyman et al., 1991).

TIRF excitation was achieved using 488-nm and 561-nm diode-pumped solid-state lasers (Melles Griot) to visualize FRA1(707)-GFP and rhodamine-labeled microtubules respectively. Images were collected with a back illuminated electron-multiplying CCD camera (Hamamatsu, ImageEM) using time-lapse capture at 1-sec intervals in the GFP channel. Kymograph analysis was conducted using Slidebook 5.0 (Intelligent Imaging Innovations). Curve fitting was conducted using KaleidaGraph (Synergy Software).

Photobleaching experiment

2 nM of FRA1(707)-GFP were immobilized on rhodamine-labeled microtubules in the presence 1mM AMPPNP and images were continuously captured to increase the rate of photobleaching. The fluorescence intensity over time of individual FRA1(707)-GFP spots was tracked using Slidebook 5.0 (Intelligent Imaging Innovations).

ACKNOWLEDGEMENTS

C.Z. was supported by grant 5T90 DA022781 from the imaging sciences pathway at Washington University. We thank the Pakrasi lab for access to the plate reader for the ATPase experiment. We thank Erica Fishel for critical reading of this manuscript and Amanda Tulin for her help with cloning FRA1.

FIGURE LEGENDS

Figure 1. Microtubule binding and ATPase activity of FRA1(707)-GFP. (A) The functional domains of FRA1 and FRA1(707)-GFP (top) and predicted coiled-coil domains of FRA1

(bottom). The FRA1 sequence was analyzed for coiled-coil formation using the MultiCoil program. (B) SDS-PAGE shows the supernatant (s) and pellet (p) fractions from a microtubule co-sedimentation assay. The ladder, FRA1(707)-GFP (106 kDa) and tubulin (55 kDa) are shown. FRA1(707)-GFP protein is mostly soluble in the absence of microtubules (lanes 1 and 2); FRA1(707)-GFP protein partitions to the pellet in the presence of 5μM microtubules (lanes 3 and 4); The addition of 5mM ATP significantly reduces the binding of FRA1(707)-GFP to microtubules (lanes 5 and 6); The addition of 5mM AMPPNP (a non-hydrolyzable analog of ATP) prevents the release of FRA1(707)-GFP from microtubules (lanes 7 and 8). (C) Microtubule concentration dependence of the ATPase activity of FRA1(707)-GFP. The ATPase activity of FRA1(707)-GFP is increased by 37-fold in the presence of microtubules. Each point represents the mean ± S.D. from three independent experiments.

Figure 2. Single molecule imaging of FRA1(707)-GFP motility. (A) Schematic of the motility assay. Rhodamine-labeled microtubules are bound to a coverslip via anti-tubulin antibody to provide tracks for kinesin movement. The rest of the glass surface is coated with pluronic F-127 polymer to block nonspecific protein binding. FRA1(707)-GFP is then flowed in along with 1mM ATP to assay motility. (B) A montage showing the movement of a single FRA1(707)-GFP molecule (yellow arrowhead) along a rhodamine-labeled microtubule (red track). Scale bar = 3 μm. (C) Kymograph showing the movement of several individual FRA1(707)-GFP molecules moving along a single microtubule (vertical bar = 20 s; horizontal bar = 1 μm). Each diagonal trace represents a motile event. (D) The velocity distribution of FRA1(707)-GFP molecules. The average velocity is 0.40 ± 0.01 μm/s (n = 320 molecules). (E) The run length distribution FRA1(707)-GFP molecules. The average run length is 3.45 ± 0.24 μm (n = 219 molecules).

Figure 3. The directionality of FRA1(707)-GFP movement on a polarity-labeled microtubule. In this montage, the brightly labeled portion to the right is the microtubule seed which initiates new growth. In the presence of dimly labeled NEM-tubulin, growth occurs mainly from the plus-end while minus-end growth is inhibited. Movement of FRA1(707)-GFP (yellow arrowhead) is always plus-end directed in these experiments (n = 30 molecules).

Figure 4. The oligomeric status of FRA1(707)-GFP. (A) Example traces of fluorescence intensity over time of individual FRA1(707)-GFP molecules that were bound to microtubules in the presence of 1mM AMPPNP (red and green traces). The purple trace represents the background fluorescence intensity in the same field of observation. (B) A bar graph of the number of bleach steps observed for 237 FRA1(707)-GFP and 288 HsKin1-GFP molecules. HsKin1-GFP is a conventional kinesin from Human that is known to work as a dimer. The few molecules showing 3 or more photobleaching steps may represent either non-specific protein aggregates or 2 or more motors that cannot be optically resolved.

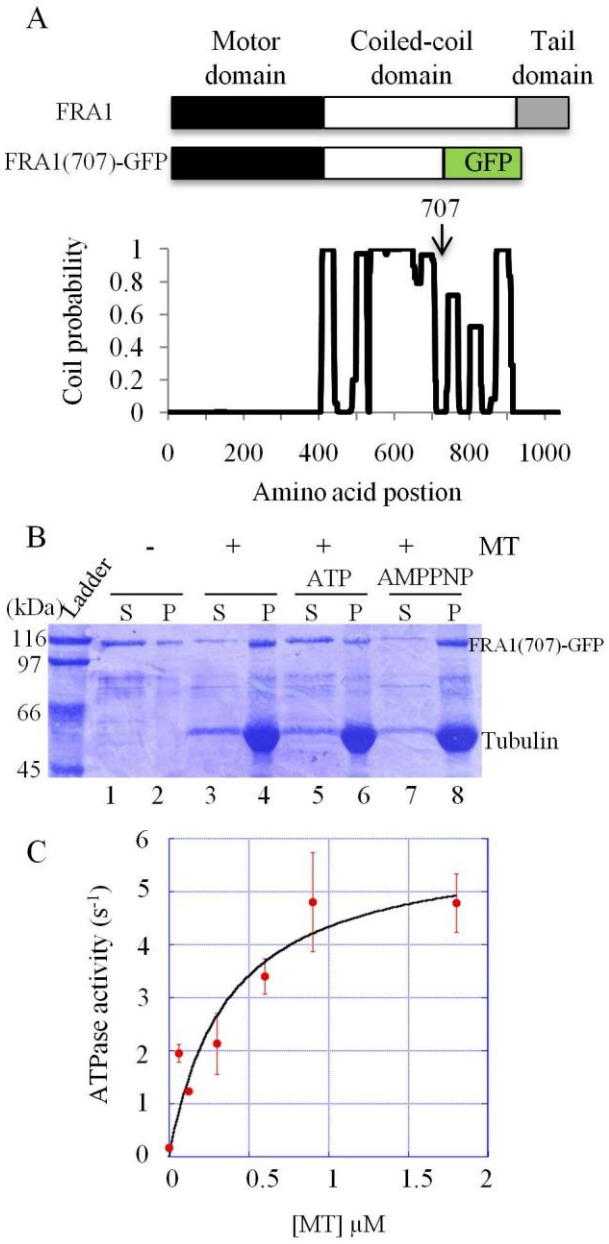

Figure 1. Microtubule binding and ATPase activity of FRA1(707)-GFP. (A) The functional domains of FRA1 and FRA1(707)-GFP (top) and predicted coiled-coil domains of FRA1 (bottom). The FRA1 sequence was analyzed for coiled-coil formation using the MultiCoil program. (B) SDS-PAGE shows the supernatant (s) and pellet (p) fractions from a microtubule co-sedimentation assay. The ladder, FRA1(707)-GFP (106 kDa) and tubulin (55 kDa) are shown. FRA1(707)-GFP protein is mostly soluble in the absence of microtubules (lanes 1 and 2);

FRA1(707)-GFP protein partitions to the pellet in the presence of 5μM microtubules (lanes 3 and 4); The addition of 5mM ATP significantly reduces the binding of FRA1(707)-GFP to microtubules (lanes 5 and 6); The addition of 5mM AMPPNP (a non-hydrolyzable analog of ATP) prevents the release of FRA1(707)-GFP from microtubules (lanes 7 and 8). (C) Microtubule concentration dependence of the ATPase activity of FRA1(707)-GFP. The ATPase activity of FRA1(707)-GFP is increased by 37-fold in the presence of microtubules. Each point represents the mean ± S.D. from three independent experiments.

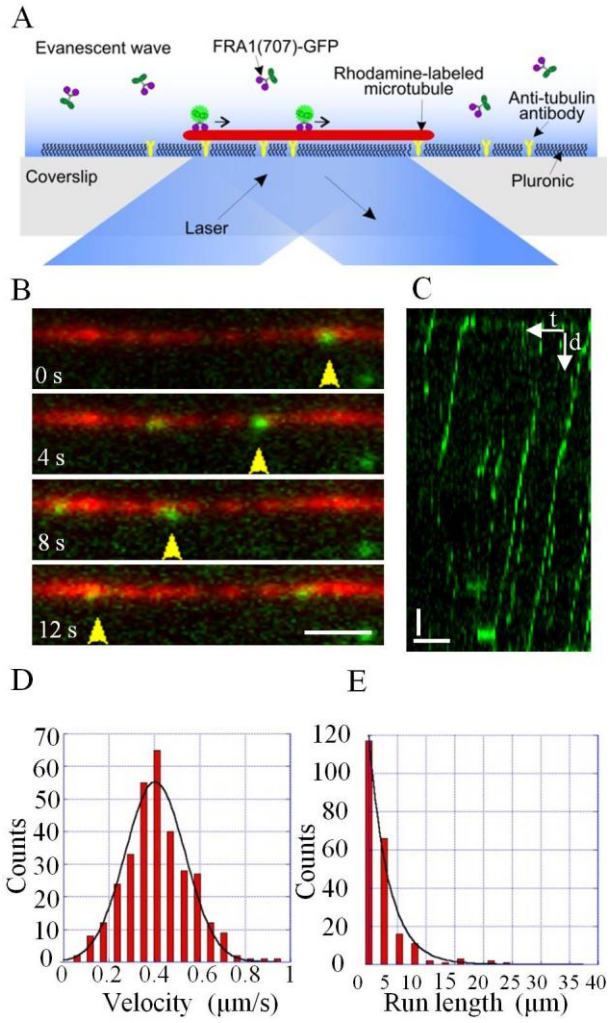

Figure 2. Single molecule imaging of FRA1(707)-GFP motility. (A) Schematic of the motility assay. Rhodamine-labeled microtubules are bound to a coverslip via anti-tubulin antibody to provide tracks for kinesin movement. The rest of the glass surface is coated with pluronic F-127 polymer to block nonspecific protein binding. FRA1(707)-GFP is then flowed in along with 1mM ATP to assay motility. (B) A montage showing the movement of a single FRA1(707)-GFP molecule (yellow arrowhead) along a rhodamine-labeled microtubule (red track). Scale bar = 3 μm. (C) Kymograph showing the movement of several individual FRA1(707)-GFP molecules moving along a single microtubule (vertical bar = 20 s; horizontal bar = 1 μm). Each diagonal trace represents a motile event. (D) The velocity distribution of FRA1(707)-GFP molecules. The average velocity is 0.40 ± 0.01 μm/s (n = 320 molecules). (E) The run length distribution FRA1(707)-GFP molecules. The average run length is 3.45 ± 0.24 μm (n = 219 molecules).

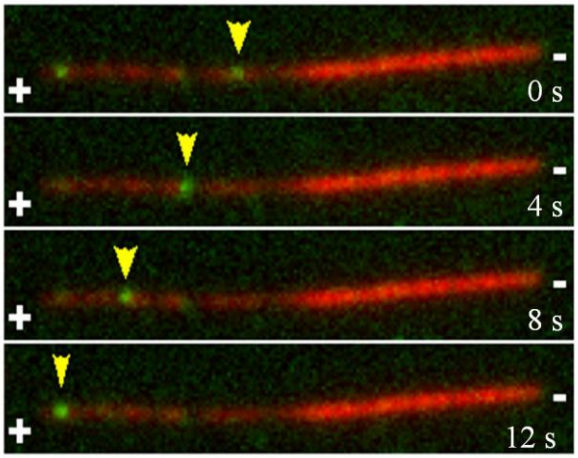

Figure 3. The directionality of FRA1(707)-GFP movement on a polarity-labeled microtubule. In this montage, the brightly labeled portion to the right is the microtubule seed which initiates new growth. In the presence of dimly labeled NEM-tubulin, growth occurs mainly from the plus-end while minus-end growth is inhibited. Movement of FRA1(707)-GFP (yellow arrowhead) is always plus-end directed in these experiments (n = 30 molecules).

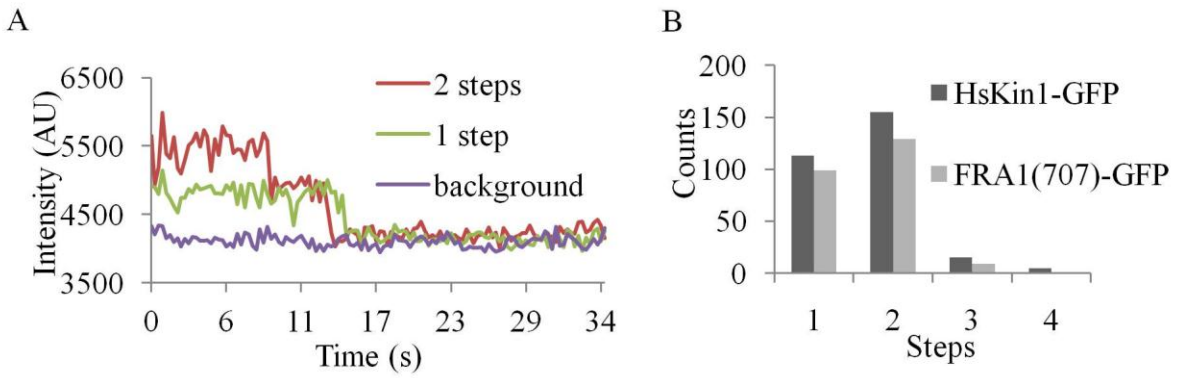

Figure 4. The oligomeric status of FRA1(707)-GFP. (A) Example traces of fluorescence intensity over time of individual FRA1(707)-GFP molecules that were bound to microtubules in the presence of 1mM AMPPNP (red and green traces). The purple trace represents the background fluorescence intensity in the same field of observation. (B) A bar graph of the number of bleach steps observed for 237 FRA1(707)-GFP and 288 HsKin1-GFP molecules. HsKin1-GFP is a conventional kinesin from human that is known to work as a dimer. The few molecules showing 3 or more photobleaching steps may represent either non-specific protein aggregates or 2 or more motors that cannot be optically resolved.

REFERENCES

Adio, S., Reth, J., Bathe, F., and Woehlke, G. (2006). Review: regulation mechanisms of Kinesin-1. J Muscle Res Cell Motil 27:153-160.

Baskin, T.I. (2001). On the alignment of cellulose microfibrils by cortical microtubules: a review and a model. Protoplasma 215:150-171.

Baskin, T.I. (2005). Anisotropic expansion of the plant cell wall. Annu Rev Cell Dev Biol 21:203-222.

Bisbal, M., et al. (2009). KIF4 mediates anterograde translocation and positioning of ribosomal constituents to axons. J Biol Chem 284:9489-9497.

Case, R.B., Rice, S., Hart, C.L., Ly, B., and Vale, R.D. (2000). Role of the kinesin neck linker and catalytic core in microtubule-based motility. Curr Biol 10:157-160.

Cosgrove, D.J. (2005). Growth of the plant cell wall. Nat Rev Mol Cell Biol 6:850-861.

Crowell, E.F., et al. (2009). Pausing of Golgi bodies on microtubules regulates secretion of cellulose synthase complexes in Arabidopsis. Plant Cell 21:1141-1154.

Crowell, E.F., Gonneau, M., Stierhof, Y.D., Hofte, H., and Vernhettes, S. (2010). Regulated trafficking of cellulose synthases. Curr Opin Plant Biol 13:700-705.

Diotallevi, F., and Mulder, B. (2007). The cellulose synthase complex: a polymerization driven supramolecular motor. Biophys J 92:2666-2673.

Endler, A., and Persson, S. (2011). Cellulose Synthases and Synthesis in Arabidopsis. Mol Plant.

Geisler, D.A., Sampathkumar, A., Mutwil, M., and Persson, S. (2008). Laying down the bricks: logistic aspects of cell wall biosynthesis. Curr Opin Plant Biol 11:647-652.

Gunawardena, S., and Goldstein, L.S. (2004). Cargo-carrying motor vehicles on the neuronal highway: transport pathways and neurodegenerative disease. J Neurobiol 58:258-271.

Gutierrez, R., Lindeboom, J.J., Paredez, A.R., Emons, A.M., and Ehrhardt, D.W. (2009). Arabidopsis cortical microtubules position cellulose synthase delivery to the plasma membrane and interact with cellulose synthase trafficking compartments. Nat Cell Biol 11:797-806.

Harada, T., and Cote, W.A. (1985). Structure of wood. In: Biosynthesis and biodegradation of wood components.--Higuchi, T., ed. San Diego: Academic Press. 1-42.

Herth, W. (1980). Calcofluor white and Congo red inhibit chitin microfibril assembly of Poterioochromonas: evidence for a gap between polymerization and microfibril formation. J Cell Biol 87:442-450.

Hirokawa, N., and Takemura, R. (2005). Molecular motors and mechanisms of directional transport in neurons. Nat Rev Neurosci 6:201-214.

Hyman, A., et al. (1991). Preparation of modified tubulins. Methods Enzymol 196:478-485.

Kuznetsov, S.A., and Gelfand, V.I. (1986). Bovine brain kinesin is a microtubule-activated ATPase. Proc Natl Acad Sci U S A 83:8530-8534.

Lasek, R.J., and Brady, S.T. (1985). Attachment of transported vesicles to microtubules in axoplasm is facilitated by AMP-PNP. Nature 316:645-647.

Lee, Y.R., and Liu, B. (2004). Cytoskeletal motors in Arabidopsis. Sixty-one kinesins and seventeen myosins. Plant Physiol 136:3877-3883.

Li, J., et al. (2011). Mutation of rice BC12/GDD1, which encodes a kinesin-like protein that binds to a GA biosynthesis gene promoter, leads to dwarfism with impaired cell elongation. Plant Cell 23:628-640.

Lloyd, C., and Chan, J. (2008). The parallel lives of microtubules and cellulose microfibrils. Curr Opin Plant Biol 11:641-646.

Lucas, J., and Shaw, S.L. (2008). Cortical microtubule arrays in the Arabidopsis seedling. Curr Opin Plant Biol 11:94-98.

Martinez, N.W., Xue, X., Berro, R.G., Kreitzer, G., and Resh, M.D. (2008). Kinesin KIF4 regulates intracellular trafficking and stability of the human immunodeficiency virus type 1 Gag polyprotein. J Virol 82:9937-9950.

Paredez, A.R., Somerville, C.R., and Ehrhardt, D.W. (2006). Visualization of cellulose synthase demonstrates functional association with microtubules. Science 312:1491-1495.

Ross, J.L., and Dixit, R. (2010). Multiple color single molecule TIRF imaging and tracking of MAPs and motors. Methods Cell Biol 95:521-542.

Sandhu, A.P., Randhawa, G.S., and Dhugga, K.S. (2009). Plant cell wall matrix polysaccharide biosynthesis. Mol Plant 2:840-850.

Shastry, S., and Hancock, W.O. (2010). Neck linker length determines the degree of processivity in kinesin-1 and kinesin-2 motors. Curr Biol 20:939-943.

Svoboda, K., and Block, S.M. (1994). Force and velocity measured for single kinesin molecules. Cell 77:773-784.

Szymanski, D.B., and Cosgrove, D.J. (2009). Dynamic coordination of cytoskeletal and cell wall systems during plant cell morphogenesis. Curr Biol 19:R800-811.

Thorn, K.S., Ubersax, J.A., and Vale, R.D. (2000). Engineering the processive run length of the kinesin motor. J Cell Biol 151:1093-1100.

Vale, R.D. (2003). The molecular motor toolbox for intracellular transport. Cell 112:467-480.

Vale, R.D., Funatsu, T., Pierce, D.W., Romberg, L., Harada, Y., and Yanagida, T. (1996). Direct observation of single kinesin molecules moving along microtubules. Nature 380:451-453.

Vale, R.D., and Milligan, R.A. (2000). The way things move: looking under the hood of molecular motor proteins. Science 288:88-95.

Valentine, M.T., and Block, S.M. (2009). Force and premature binding of ADP can regulate the processivity of individual Eg5 dimers. Biophys J 97:1671-1677.

Verhey, K.J., and Hammond, J.W. (2009). Traffic control: regulation of kinesin motors. Nat Rev Mol Cell Biol 10:765-777.

Wasteneys, G.O., and Ambrose, J.C. (2009). Spatial organization of plant cortical microtubules: close encounters of the 2D kind. Trends Cell Biol 19:62-71.

Wightman, R., and Turner, S. (2010). Trafficking of the plant cellulose synthase complex. Plant Physiol 153:427-432.

Woehlke, G., and Schliwa, M. (2000). Walking on two heads: the many talents of kinesin. Nat Rev Mol Cell Biol 1:50-58.

Wu, G., et al. (2008). A novel role of the chromokinesin Kif4A in DNA damage response. Cell Cycle 7:2013-2020.

Zhang, M., et al. (2010). Brittle Culm 12, a dual-targeting kinesin-4 protein, controls cell-cycle progression and wall properties in rice. Plant J 63:312-328.

Zhong, R., Burk, D.H., Morrison, W.H., 3rd, and Ye, Z.H. (2002). A kinesin-like protein is essential for oriented deposition of cellulose microfibrils and cell wall strength. Plant Cell 14:3101-3117.

Zhu, C., and Jiang, W. (2005). Cell cycle-dependent translocation of PRC1 on the spindle by Kif4 is essential for midzone formation and cytokinesis. Proc Natl Acad Sci U S A 102:343-348.